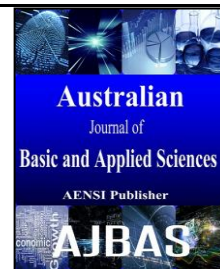




ISSN:1991-8178

Australian Journal of Basic and Applied Sciences

Journal home page: www.ajbasweb.com



Fabrication of GPS Patch Antennas Based on Microwave Dielectric Ceramics $Zn_{(1-x)}Co_xAl_2O_4$ Thin Film by Sol Gel Method

Huda Abdullah, Wan Nasarudin Wan Jalal and Mohd Syafiq Zulfakar

Department of Electrical, Electronic and System Engineering, Faculty of Engineering and Built Environment, Universiti Kebangsaan Malaysia, 43600 Bangi, Selangor, Malaysia

ARTICLE INFO

Article history:

Received 13 November 2013

Accepted 23 October 2013

Available online 30 November 2011

Keywords:

$ZnAl_2O_4$, GPS antenna, Dielectric constant, Antennas performance

ABSTRACT

Background: The microwave dielectric properties of $Zn_{(1-x)}Co_xAl_2O_4$ thin films were examined with a view to their exploitation for GPS antenna. The $Zn_{(1-x)}Co_xAl_2O_4$ thin films were prepared by the sol gel method at 500 °C for 1 h. Co addition decreased the crystallite size and surface morphology of the resultant films, evidently affecting their density and dielectric constant (ϵ_r). Based on the material investigated and microwave antenna theory, GPS patch antennas were fabricated using $Zn_{(1-x)}Co_xAl_2O_4$ and then studied using a PNA series network analyzer. The measured results show that antennas had the return loss and impedance bandwidths of -16.6 to -20.3 dB and 75–180 MHz, respectively. The GPS patch antenna fabricated from $Zn_{0.85}Co_{0.15}Al_2O_4$ showed an excellent combination between the return loss (-20.3 dB), small in size (4.68 x 3.13 cm²) and wide bandwidth (180 MHz).

© 2015 AENSI Publisher All rights reserved.

To Cite This Article: Huda Abdullah, Wan Nasarudin Wan Jalal and Mohd Syafiq Zulfakar., Fabrication of GPS Patch Antennas Based on Microwave Dielectric Ceramics $Zn_{(1-x)}Co_xAl_2O_4$ Thin Film by Sol Gel Method. *Aust. J. Basic & Appl. Sci.*, 9(12): 31-36, 2015

INTRODUCTION

Microstrip antennas are attractive due to their light weight, conformability and low cost. These antennas can be integrated with printed strip-line feed networks and active devices. This is a relatively new area of antenna engineering. The application of this type of antennas started in early 1970s when conformal antennas were required for use in missiles. A major contributing factor for recent advances of microstrip antennas is the current revolution in electronic circuit miniaturization brought about by developments in large scale integration. A microstrip antenna consists of conducting patch on a ground plane separated by dielectric substrate. This concept was undeveloped until the revolution in electronic circuit miniaturization and large scale integration in 1970. After that many authors have described the radiation from the ground plane by a dielectric substrate for different configurations. Low dielectric constant substrates are generally preferred for maximum radiation. However this technique has also limitation the miniature size of microstrip antenna. Such researchers preferred to use the material that has high dielectric constant as conducting patch material especially for global positioning system (GPS) application. This technique can be achieved by using the microwave dielectric material (Abdullah *et al.* 2014; Jalal *et al.* 2014). Miniaturization of

patch antennas for volume efficiency in GPS applications has become a primary issue in these few years. In particular, materials with high dielectric constant can reduce the antenna size. Several research efforts have recently been dedicated toward the development of such dielectric materials (Huang *et al.* 2009).

Among that kind of microwave dielectric material, the nanostructured transition metal-oxide spinels are good potential to develop as GPS antenna. This is because of their low temperature sinterability, high thermal resistance, and increased hardness (Kumar *et al.* 2012); these properties make spinels promising catalytic or carrier materials and precursors for mixed oxides. Spinel has enormous potential to generate well-dispersed, active, and very stable catalysts. Zinc aluminate ($ZnAl_2O_4$) and cobalt aluminate ($CoAl_2O_4$) have a normal spinel type structure of the general formula AB_2O_4 . The $ZnAl_2O_4$ ceramics have been reported to have good dielectric properties and have been of great interest as a potential dielectric resonator for millimeter-wave applications in the last decade (Surendran *et al.* 2004). However, till now, no report is available on the successfully fabrication of a material such as $ZnAl_2O_4$ doped with cobalt (Co) for use as GPS patch antenna.

In this study, the microwave dielectric properties of $ZnAl_2O_4$ spinels were determined. Tailoring of

ZnAl₂O₄ spinel properties was performed by molar mixing with Co to form Zn_(1-x)Co_xAl₂O₄ and develop an alternate microwave dielectric ceramic for GPS antennas. The microstrip patch antenna for GPS application was fabricated and its performance was measured.

Experimental Procedure:

The zinc acetate dehydrate Zn(O₂CCH₃)₂, aluminium nitrate nonahydrate Al(NO₃)₃·9H₂O and cobalt (II) acetate tetrahydrate Co(CH₃COO)₂·4H₂O were dissolved in absolute ethanol (C₂H₅OH). The substitution of Zn²⁺ by Co²⁺ in the framework of ZnAl₂O₄ was prepared by the sol gel method with different concentration (*x*) of Co (*x* = 0.00, 0.05, 0.15 and 0.25). Initially aluminium nitrate was dissolved in 60 ml absolute ethanol (C₂H₅OH), followed by ethylene glycols (EG) with designated amount (0.5 ml) as the chelating agent. Afterwards, the Co(CH₃COO)₂·4H₂O and Zn(O₂CCH₃)₂ were added to the solution. After being kept at around 75 °C for 1 h, the nitric acid (CA) with amount 0.36 ml are utilized for preparing homogeneous solution. The solution was continuously heated at 75 °C with constant stirring on a magnetic stirrer for another 1 h until a clear solution had taken place following a chemical reaction. Finally, the solution containing of Zn_(1-x)Co_xAl₂O₄ is stirred for 0.5 h at 180 °C in order to obtain transparent and stable sol.

Furthermore, Zn_(1-x)Co_xAl₂O₄ thin films have been deposited using sol-gel spin coating technique. The transparent and stable sol of Zn_(1-x)Co_xAl₂O₄ would be prepared on the fluorine tin oxide (FTO) substrate by the spin coating technique at 3500 rpm/min for 35 s and treated at 85 °C for 15 min. These coating procedures were repeated 10 times to get a result of good thickness and to remove the organic residuals. The thin films were annealed at 700 °C for 1 h (1°C/min) to eliminating the remaining organic matter.

The nanostructure of ZnAl₂O₄ doped Co was characterized by means of the X-ray diffraction (XRD) method. The density of the annealed thin films was measured by the Archimedes method. The surface morphology of thin films was observed by Atomic Force Microscope (AFM, NTEGRA Prima). The ε_r values were measured using an LCR spectrometer (HP 4284A) at frequency range 20 Hz to 1 MHz at room temperature. Finally, the patch antennas were successfully fabricated on the FTO substrate and then, measured their return loss by the PNA series network analyzer (E8358A, Agilent).

RESULTS AND DISCUSSION

X-ray diffraction studies (XRD):

The XRD patterns of the Zn_(1-x)Co_xAl₂O₄ thin films system annealed at 500 °C for 1 h are shown in Fig. 1. As the *x* value increases, the peaks in the XRD spectra shift to a higher angle implying the

formation of solid solution. Analysis of the XRD pattern depicted the formation of the main crystalline planes (220), (222), (400), (331) (422) and (511) at 2θ = 31.72°, 37.78°, 44.78°, 47.51°, 56.64° and 59.34°, respectively and it was proven that (311) is the preferential orientation, as previously reported by Barros *et al.* (Barros *et al.* 2006). The peaks corresponding to CoAl₂O₄ (JCPDS File Card No. 00-044-0160) show the same peaks as ZnAl₂O₄ (JCPDS File Card No. 00-005-0669). The peaks shift to a higher angle because the ionic radius of Co²⁺ (0.58 Å) (Huang *et al.* 2008) is smaller than that of Zn²⁺ (0.74 Å) (Park *et al.* 2012). The observed diffraction peaks of all samples correspond to the standard pattern of face-centered cubic ZnAl₂O₄ with dominant peak (311) at around 36.26°. However, at *x*=0.05, the XRD patterns also show that the presence of secondary phases corresponding to the hexagonal ZnO and appear as crystalline planes (100), (002), (101), (102) and (110). These phenomena were also explained by Renata and Osvaldo (2010). The formation of the secondary phases was attributed to the formation of vacancies resulting from the incorporation of Co ions into the host lattice (ZnAl₂O₄). Therefore, at *x* = 0.05, the highest diffraction peaks observed at (220) due to Co²⁺ ions may be substitute with the trivalent Al³⁺ ions or divalent Zn²⁺ ions. From the most intense peak, only peak (220) and (311) was observed as spinel structures. The nature of the Co²⁺ ions doping the nanostructured ZnAl₂O₄ spinels appears to be much complex, for it is possible that these ions substitute the trivalent Al³⁺ ions or divalent Zn²⁺ ions. However, the peak changed back to (311) with the increase of Co amount and form as solid solution spinel structured (Zn/CoAl₂O₄).

The crystallite size was calculated from the broadening peak (311) of the XRD data using Scherrer's equation:

$$D = 0.94 (\lambda / (\beta \cos \theta)) \quad (1)$$

where λ is the X-ray wavelength (0.15418 nm) and β is the full-width at half maximum intensity of the diffraction line. By increasing the amount of Co loading, the crystallite size decreases linearly from 14.65 nm to 7.56 nm, except at *x* = 0.05 (15.48). The increased in crystallite size at *x* = 0.05 due to ZnO was observed. The reduction in crystallite size may be due to the high energy required by Co²⁺ ions to enter the lattice host and get substituted for complete grain crystallization and growth. Furthermore, the large degree of disorder the ions produce in the lattice host as a result of ionic radius mismatches between Co²⁺, Zn²⁺, and Al³⁺ ions (Kumar *et al.* 2012) also decreased the crystallite size (Abdullah *et al.* 2014).

The lattice parameter of ZnAl₂O₄ was calculated based on the X-ray diffraction patterns, using equation below (Ianoş *et al.* 2012):

$$a = d_{hkl} (h^2 + k^2 + l^2) \quad (2)$$

The experimental values of lattice parameters (a) upon the Ca-substitution of Zn increased from 8.085 to 8.12 Å, except at $x = 0.05$ ($a = 8.06$ Å). The increase in a was attributed to the peak shifted to the higher angle. The shift of XRD diffraction peaks was indicated that the a has changed. These experimental

lattice parameters of ZnAl_2O_4 are in good agreement with the reported value $a = 8.083$ to 8.095 Å (Luiz *et al.* 2009; Zawadzki *et al.* 2009) (Abdullah *et al.* 2014; C. *et al.* 2009; Zawadzki *et al.* 2009) and the theoretical value (8.05 Å).

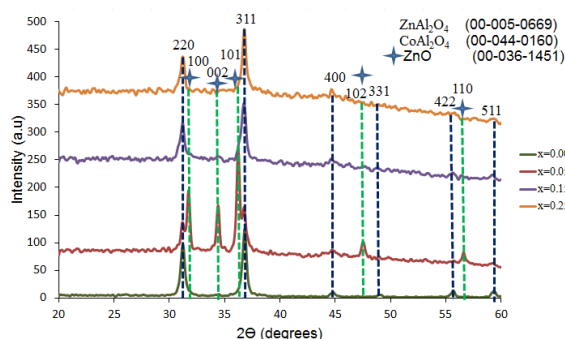


Fig. 1: The XRD patterns of the $\text{Zn}_{(1-x)}\text{Co}_x\text{Al}_2\text{O}_4$ thin films annealed at 500 °C for 1 h.

FTIR analysis:

The FT-IR spectra of $\text{Ti}_x\text{Zn}_{(1-x)}\text{Al}_2\text{O}_4$ thin films is shown in Fig. 3. All the spectra exhibit a common broad band near 3519 cm^{-1} and near 1894 cm^{-1} due to the $-\text{OH}$ stretching vibrations and deformative vibration of water molecules respectively. The band at 2328 cm^{-1} can be attributed to the presence of oxygen bonds in the face-centred cubic crystal lattice of oxygen atoms. This peak is observed in all spinel compounds and can be treated as a characteristic feature of spinel structures (Wan Jalal *et al.* 2013).

The spectra of all the samples showed the peak at 1400 cm^{-1} which assigned to the Al-O stretching vibrations. The metal-oxygen stretching frequencies in the range $400\text{--}1000\text{ cm}^{-1}$ are related to the inorganic network. The bands around 490, 560 and 650 cm^{-1} are characteristic of $\text{Co/ZnAl}_2\text{O}_4$ spinel. These bands correspond to the bending mode of ZnO , CoO and AlO_6 which is the built up of $\text{Co/ZnAl}_2\text{O}_4$ compound and indicates the final formation for all the prepared thin film samples.

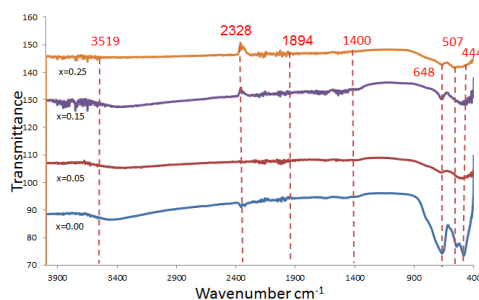


Fig. 2: FTIR analysis of $\text{Zn}_{(1-x)}\text{Co}_x\text{Al}_2\text{O}_4$ thin films annealed at 500 °C for 1 h.

Morphological Observation:

The atomic force microscopy (AFM) was used to analyze the surface morphology of $\text{Zn}_{(1-x)}\text{Co}_x\text{Al}_2\text{O}_4$ thin films as shown in Fig. 2. The scanning size was $1 \times 1\ \mu\text{m}^2$. The surface roughness average (rms) of ZnAl_2O_4 , $\text{Zn}_{0.95}\text{Co}_{0.05}\text{Al}_2\text{O}_4$, $\text{Zn}_{0.85}\text{Co}_{0.15}\text{Al}_2\text{O}_4$, and $\text{Zn}_{0.75}\text{Co}_{0.25}\text{Al}_2\text{O}_4$ thin films were observed as 15.07, 33.47, 9.18 and 6.33 nm, respectively. The doped samples (Fig. 2c–d) had smoother surface areas compared with ZnAl_2O_4 (Fig. 2a) due to the fact that grain and crystallite size were decreased. However, the higher in surface roughness occur at $x = 0.05$ (33.5 nm), due to secondary phases (ZnO) appear. The secondary phases (ZnO) appear on surface

morphology, at $x = 0.05$, which is in agreement with XRD data. The decrease of surface roughness can affect the ceramics density and ϵ_r (Jalal *et al.* 2014).

Dielectric Properties:

The apparent densities and ϵ_r of $\text{Zn}_{(1-x)}\text{Co}_x\text{Al}_2\text{O}_4$ thin films as shown in Fig. 3. The density of the annealed thin films was measured by the Archimedes method from XRD data from XRD data. The density of annealed pure ZnAl_2O_4 was measured to be 4.61 g/cm^3 which is slightly higher than its theoretical density (4.58 g/cm^3) (Müller-Buschbaum 2003). Initially, the density apparently decreases with increasing x concentration. However, after reaching

its maximum 4.64 g/cm^3 at $x = 0.05$, and it starts to decrease until 4.56 g/cm^3 at $x = 0.25$. The decreases in densities can be expected because the density of CoAl_2O_4 (4.416 g/cm^3) (Lee *et al.* 2009) is lower than that of ZnAl_2O_4 (4.58 g/cm^3) (Müller-Buschbaum 2003). The increase in the density at $x = 0.05$ is due to the larger crystallite size and the secondary phases (ZnO) occurred as observed in Fig. 2a. Normally, the increase in apparent densities contributed to the increment of dielectric constant and plays an important role in order to miniaturize GPS patch antennas (Jalal *et al.* 2014). Furthermore, the increase in density may be caused by the decrease

in the number of pores and a decrease in relative density may be caused by the porous nanostructure (Chen 2011). Chen (Chen 2011) and Huang *et al.* (Huang *et al.* 2009) reported, the increase in apparent densities was associated with high dielectric constant and played an important role in controlling the dielectric loss for GPS patch antenna. The decreased in densities is attributed to the increase in volume ratio of CoAl_2O_4 phase and decrease in volume ratio of ZnAl_2O_4 phase, which indicates that the particles in the $(\text{Co/Zn})\text{Al}_2\text{O}_4$ film are compact and more uniform.

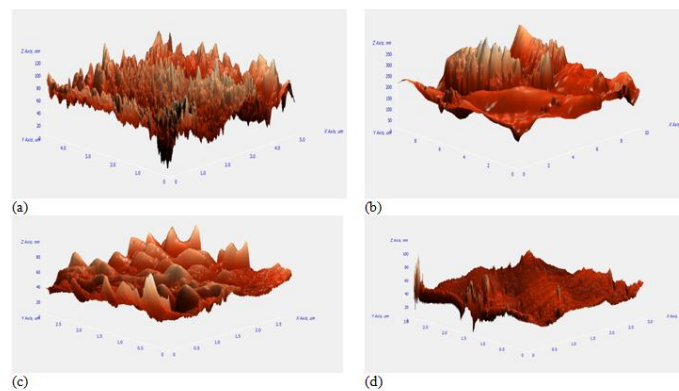


Fig. 3: AFM images of $\text{Zn}_{(1-x)}\text{Co}_x\text{Al}_2\text{O}_4$ thin films (a) $x=0.00$, (b) $x=0.05$, (c) $x=0.15$ and (d) $x=0.25$.

The ϵ_r values of well-annealed $\text{Zn}_{(1-x)}\text{Co}_x\text{Al}_2\text{O}_4$ films range from 6.08 to 12.28. The highest value of $\epsilon_r \sim 12.28$ was obtained at the composition $x = 0.05$ and decreased slowly at $x=0.15, 0.25$ as Co increases. The obtained dielectric constant of pure ZnAl_2O_4 ceramics was 8.56. The ϵ_r value increased at $x =$

0.05 could be related to the afore-mentioned porous morphology due to ZnO observed. Fig. 3 also shows that the variation of dielectric constant is consistent with that of density.

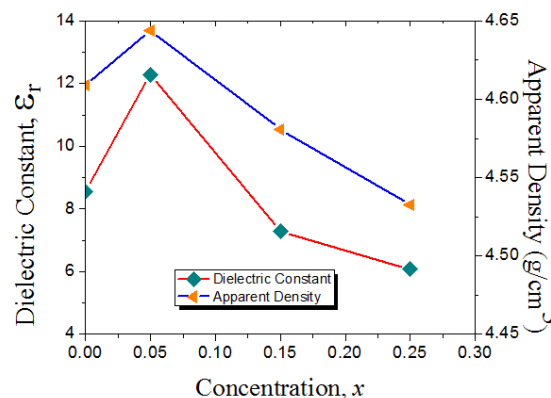


Fig. 3: Apparent density and dielectric constant of $\text{Ca}_x\text{Zn}_{(1-x)}\text{Al}_2\text{O}_4$ films as a function of Co-concentration (x).

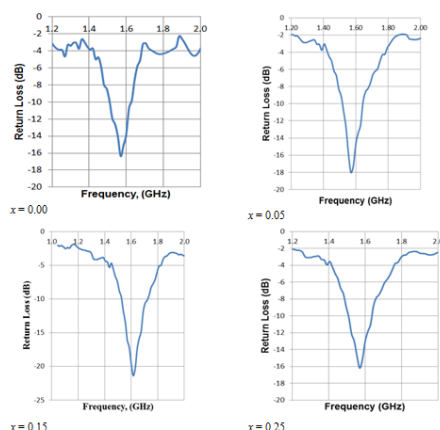
Fabricated GPS antenna and its performances:

Based on the microwave antenna theory (Balanis 2005), the microstrip patch antenna for GPS application was fabricated on FTO substrate by using the $\text{Zn}_{(1-x)}\text{Co}_x\text{Al}_2\text{O}_4$ material and then measured. The dimensions of the patch depend on the ϵ_r values of $\text{Zn}_{(1-x)}\text{Co}_x\text{Al}_2\text{O}_4$ ceramics and FTO substrates. The

results show that the materials with $\epsilon_r \sim 12.26$ decreased the patch size from $3.69 \times 2.34 \text{ cm}^2$ which is smaller than pure ZnAl_2O_4 material ($\epsilon_r \sim 8.56 \text{ cm}$, $4.36 \times 2.87 \text{ cm}^2$). Fig. 4 shows the measured return loss and bandwidth of the fabricated GPS antenna. It shows that all the antennas operate at 1.5750 GHz. The measured results also show that antennas had the

return loss and impedance bandwidths of -16.6 to -20.3 dB and 75–180 MHz, respectively, to accommodate an efficient antenna feed for GPS application. Among these antennas, the $Zn_{0.85}Co_{0.15}Al_2O_4$ showed an excellent

combination between the return loss (-20.3 dB), small in size ($4.68 \times 3.13 \text{ cm}^2$) and wide bandwidth (180 MHz). Thus, we concluded that Co is an effective dopant for $ZnAl_2O_4$ to improve the performances of GPS patch antennas.



Conclusion:

The $Zn_{(1-x)}Mg_xAl_2O_4$ microwave dielectric ceramics thin films were successfully synthesized through sol-gel method. A $Zn_{(1-x)}Co_xAl_2O_4$ solid solution with a spinel structure was observed in the $ZnAl_2O_4$ and $MgAl_2O_4$ system. The behavior of ϵ_r as a function of the composition was similar to that of density. Apparent density plays an important role in controlling the return loss of GPS antenna. The increase in apparent densities contributed to the increment of dielectric constant and plays an important role in order to miniaturize GPS patch antennas. All the fabricated GPS antennas achieved the minimum requirement of antenna specification to ensure full functionality. The $Zn_{0.85}Co_{0.15}Al_2O_4$ showed an excellent combination between the return loss (-20.3 dB), small in size ($4.68 \times 3.13 \text{ cm}^2$) and higher bandwidth (180 MHz).

ACKNOWLEDGEMENT

This work was supported by the Institute of Microengineering and Nanoelectronics (IMEN), Universiti Kebangsaan Malaysia under grant FRGS/2/2013/TK06/UKM/02/3 and ERGS/1/2012/STG05/UKM/02/5.

REFERENCES

Abdullah, H., W. Jalal, M. Zulfakar, 2014. Miniaturization of Gps Patch Antennas Based on Novel Dielectric Ceramics $Zn(1-X)Mg_xAl_2O_4$ by Sol-Gel Method. *Journal of Sol-Gel Science and Technology* 69(2): 429-440.

Balanis, C.A., 2005. *Antenna Theory Analysis and Design*. 3rd. Hoboken, New Jersey, USA: John Wiley & Sons, Inc.

Barros, B.S., P.S. Melo, R.H.G.A. Kiminami, A.C.F.M. Costa, G.F. Sá, S. Alves, Jr., 2006. Photophysical Properties of Eu^{3+} and Tb^{3+} -Doped $ZnAl_2O_4$ Phosphors Obtained by Combustion Reaction. *Journal of Materials Science*, 41(15): 4744-4748.

C., D.S.L.K., R., Z.J., N., D. R. G., B., S. L. E., G., D. S. L. M., G., S. A., Thomas, S., S., A. R. & F., D. C. C.E., 2009. *Blue Pigments Based on $Co(X)Zn(1-X)Al_2O_4$ Spinels Synthesized by the Polymeric Precursor Method*. Oxford, ROYAUME-UNI: Elsevier.

Chen, Y.C., 2011. Microwave Dielectric Properties of $(Mg(1-X)Co_x)_2SnO_4$ Ceramics for Application in Dual-Band Inverted-E-Shaped Monopole Antenna. *Ultrasonics, Ferroelectrics and Frequency Control, IEEE Transactions on*, 58(12): 2531-2538.

Huang, C.L., C.F. Tasi, Y.B. Chen, Y.C. Cheng, 2008. New Dielectric Material System of $(Mg_{0.95}Zn_{0.05})TiO_3-Ca_{0.61}Nd_{0.26}TiO_3$ at Microwave Frequency. *Journal of Alloys and Compounds*, 453(1-2): 337-340.

Huang, C. L., J.Y. Chen, B.J. Li, 2009. Characterization and Dielectric Behavior of a New Dielectric Ceramics $Ca(Mg_{1/3}Nb_{2/3})O_3-(Ca_{0.8}Sr_{0.2})TiO_3$ at Microwave Frequencies. *Journal of Alloys and Compounds*, 484(1-2): 494-497.

Ianoş, R., R. Lazău, I. Lazău, C. Păcurariu, 2012. Chemical Oxidation of Residual Carbon from $ZnAl_2O_4$ Powders Prepared by Combustion Synthesis. *Journal of the European Ceramic Society*, 32(8): 1605-1611.

Jalal, W. N. W., Abdullah, H., Zulfakar, M. S., Shaari, S., Islam, M. & Bais, B. 2014. Characteristics of Nanostructured $CaxZn(Al_2O_4)$ Thin Films Prepared by Sol-Gel Method for Gps Patch Antennas. *Sains Malaysiana*, 43(6): 833-842.

Kumar, R.T., N.C.S. Selvam, C. Ragupathi, L.J. Kennedy, J.J. Vijaya, 2012. Synthesis, Characterization and Performance of Porous Sr(Ii)-Added ZnAl₂O₄ Nanomaterials for Optical and Catalytic Applications. *Powder Technology* 224(0): 147-154.

Lee, G.Y., K.H. Ryu, H.G. Kim, Y.Y. Kim, 2009. The Preparation of Blue Coal₂O₄ Powders by the Malonate Method: The Effect of the Amount of Malonic Acid Used, the Formation Pathway of Coal₂O₄ Crystallites and the Characteristics of the Prepared Powders. *Bull. Korean Chem. Soc.*, 30(2): 373.

Müller-Buschbaum, H., 2003. The Crystal Chemistry of Am₂O₄ Oxometallates. *Journal of Alloys and Compounds*, 349(1–2): 49-104.

Park, J.H., S. Nahm, J.G. Park, 2012. Crystal Structure and Microwave Dielectric Properties of (1–X) Zn₂O₆—X₂O Ceramics. *Journal of Alloys and Compounds*, 537: 221-226.

Surendran, K.P., N. Santha, P. Mohanan, M.T. Sebastian, 2004. Temperature Stable Low Loss Ceramic Dielectrics in (1-X)ZnAl₂O₄-X₂O System for Microwave Substrate Applications. *The European Physical Journal B - Condensed Matter and Complex Systems* 41(3): 301-306.

Wan Jalal, W.N., H. Abdullah, M.S. Zulfakar, S. Shaari, M.T. Islam, 2013. Characterization and Dielectric Properties of Novel Dielectric Ceramics Ca_xZn_(1-x)Al₂O₄ for Gps Patch Antennas. *International Journal of Applied Ceramic Technology*. Doi: 10.1111/ijac.12193.

Zawadzki, M., W. Staszak, F.E. López Suárez, M.J. Illán Gómez, A. Bueno López, 2009. Preparation, Characterisation and Catalytic Performance for Soot Oxidation of Copper-Containing ZnAl₂O₄ Spinels. *Applied Catalysis A: General*, 371(1–2): 92-98.